21st Annual Conference of the Canadian Nuclear Society
Toronto, Ontario, Canada / June 11-14, 2000

Heat Transfer in a CANDU Type Fuel Bundle During a LOCA Experiment

D.J. Wallace
Atomic Energy of Canada Limited
Safety Thermalhydraulics Branch
Whiteshell Laboratories
Pinawa, Manitoba R0E 1L0
Canada

Abstract

Pre- and post-test simulations with the thermalhydraulics code CATHENA [1] (Canadian Algorithm for THErmalhydraulic Network Analysis) MOD-3.5c/Rev 0 of a LOCA (Loss of Coolant Accident) experiment in the RD-14M test facility at AECL, Whiteshell Laboratories, Canada were performed. The simulations were performed to assess the heat transfer calculations by CATHENA in a CANDU® (CANada Deuterium Uranium) type fuel bundle under conditions expected in the unlikely event of a LOCA. The experiment was a 15-mm diameter inlet-header break with a primary-pump exponential ramp-down, and no emergency-coolant injection (ECI). Two channels in the RD-14M loop were used, one per pass, with a simulated power pulse in the channel of the broken pass.

In the pre-test simulation results, average maximum sheath temperatures were 15% higher than measured temperatures. Analysis of the post-test simulation results identified uncertainties in the heat transfer correlations, flow regime, and discharge conditions as the most important factors contributing to the discrepancy between measured and simulation results. These uncertainties and their impact on the calculated fuel sheath temperatures are presented and discussed in detail in this paper.

Introduction

In a postulated LOCA in the primary heat transport loop of a CANDU reactor, coolant voiding can result in a power pulse before reactor safety shut-down systems become fully engaged. Test B9903 was conducted to provide data on a simulated LOCA in the RD-14M primary heat transport loop. More specifically, the experiment was conducted to examine the heat transfer characteristics in a CANDU type fuel bundle during a postulated LOCA with a channel power pulse and no Emergency Core Cooling (ECC) available. Pre- and post-test simulations of test B9903 were performed with the thermalhydraulics code CATHENA with the following objectives:

1) to investigate the heat transfer mechanisms of the fuel under these conditions, and
2) to assess the ability of CATHENA to capture the thermalhydraulic behaviour in the channel during the transient.

Experimental

Facility Description

The RD-14M test facility is a pressurized water loop with many of the geometric features of a CANDU reactor primary heat transport system (Figure 1), including the full vertical scale of a reactor. Many of the thermalhydraulic features of a CANDU reactor heat transport system are also included. The primary side includes four headers, two U-tube steam generators (BO1 and BO2) and ten 6 m-long horizontal channels in a figure-of -eight loop representing two passes (five channels per pass) through a CANDU reactor core. The channels, or test sections, contain electrically heated nominal 1 MW fuel element simulators (FES). Each of the FES consist of 7 pins representative of the seven central pins of a 37-element CANDU bundle. Further details on the facility and instrumentation can be found in [2,3]

Test Description

Test B9903 was conducted using a single channel per pass configuration (channels or test sections (TS) 9 and 14, Figure 1). Valves isolated channels 5 to 8, and 10 to 13 from the primary loop. The LOCA event was initiated by opening a 15 mm break valve installed in inlet header 8. A simulated power pulse in TS14, a power ramp-down in TS9, and a primary pump ramp-down were synchronised with the opening of the break valve. Nominal conditions for the test are listed in Table 1 and the sequence of events for the transient is shown in Table 2.

Numerical Model

CATHENA is a one-dimensional, two-fluid thermalhydraulic code used for the analysis of postulated LOCAs [1]. A one-step, semi-implicit method is used to solve six partial differential conservation equations represented in finite difference form over a staggered mesh. In the study reported in this paper, an idealization with approximately 300 nodes representing both the primary (Figure 2) and secondary (Figure 3) loops of the RD-14M facility was used. The nominal thermalhydraulic conditions shown in Table 1 were applied to obtain steady-state initial conditions for both the pre- and post-test simulations. Boundary conditions were imposed on the primary side by supplying a primary pump ramp-down speed and power profiles for the FES in test sections 9 and 14 (Figures 4 and 5). Boundary conditions were applied on the secondary side by providing a boiler feed-water inlet temperature, a boiler outlet pressure and a boiler level.

(a) Pre-test Simulation

The steady state thermalhydraulic conditions used to perform the pre-test simulation of the transient are shown in Table 3. The primary pump RPM speed was adjusted to achieve the desired steady state channel flows. An exponential pump ramp-down curve from a previous test (Figure 4) was used to model the primary pump speed during the transient. An estimate of the experimental power pulse for heated section 14 was made for the pre-test simulation of the transient (Figure 5). During the transient, the inlet feed-water temperature and outlet steam pressure on the secondary side were assumed constant at the initial, steady-state values. The inlet feed-water flow was calculated via a proportional-derivative control device model to maintain boiler levels of 840 mm (55%) during the transient.

(b) Post-Test Simulation

The measured and simulated thermalhydraulic steady-state conditions at the beginning of the test are shown in Table 4. The following measured parameters were used as boundary conditions in the simulated transient: primary pump ramp-down (Figure 4), test sections 9 and 14 power histories, and on the secondary side, inlet feed-water temperature, boiler outlet steam pressure and boiler inlet feed-water flow. Since steady feed-water flow at the inlet of both boilers did not occur in the experiment, the steam mass flow measured at the boiler outlets were used as the inlet feed-water flow boundary conditions. A delay time of 0.85 s was used to open the break valve in inlet header 8. This delay time was calculated from the difference between the time the signal was sent to open the valve and the time de-pressurisation in header 8 was first observed in the test data.

Results

(a) Pre-Test Simulation Results

The calculated and measured inlet flows for test section 14 are shown in Figure 6. The initial drop in the flow in response to the opening of the break occurs approximately 0.85 s earlier in the calculated than in the measured flow. Immediately after the break is initiated (at 0.0 s), the calculated flow in the test section shows a brief flow stagnation at 0.2 s, with a flow reversal at the inlet end beginning at 1.3 s. The measured results show a reversal in flow at this location at 3.1 s. At 10 s the calculated inlet flow decreases temporarily to -16 L/s, much lower than the experimental threshold of -7 L/s. The peak sheath temperatures are shown for the outlet end of the top pin (Figure 7) of the test section 14. The maximum difference between the calculated (620°C) and measured (512°C) sheath temperature for the channel occurred at this location.

(b) Post-Test Simulation Results

A comparison of Figures 8 and 9 shows the effect of including a delay time of 0.85 s in the opening of the header 8 break valve. Flow reversal in test section 14 occurs at 2.4 s in the post-test simulation compared to 3.1 s in the experiment (Figure 9), and 1.3 s in the pre-test simulation (Figure 8). The improved estimate in the timing of flow reversal (by 1.1 s) is largely attributed to the 0.85 s valve delay time applied in the post-test simulation. The calculated peak sheath temperature of 620°C at the outlet end of the top pin shown in Figure 9 for the post-test simulation is lower than the temperature obtained with the pre-test simulation (631°C) but still significantly higher than the measured temperature of 512°C at the same location.

Discussion

The post-test calculated peak sheath temperature of the top pin at the outlet end of test section 14 (HS14) was higher than the measured temperature by 108°C. A more complete picture of the calculated sheath temperature can be obtained by examining the axial distribution of the sheath temperature. Measured and calculated top pin sheath temperature histories at various axial locations are shown in Figures 10 and 11. The top pin temperatures are discussed in this paper because differences between the measured and calculated sheath temperatures were greater for the top pins, than for the middle or lower pins. Comparison of the temperatures in Figures 10 and 11 shows a smaller axial variation in the maximum measured axial temperatures than the maximum calculated sheath temperatures. The axial set of maximum measured temperatures gave an average temperature of 508°C with a corresponding standard deviation of 10°C. The average temperature calculated in this way will be referred to as an "average maximum" temperature. The average maximum for the calculated temperatures was 581°C, with a standard deviation of 30°C. A preliminary assessment showed uncertainties in the calculated results were the greatest in the following parameters: heat-transfer correlation, flow regime transition from single-phase liquid to two-phase flow (i.e., mixed or stratified), and break discharge (break discharge area and coefficient). These parameters were then investigated to determine their impact on the average maximum and standard deviation of the calculated top pin sheath temperature. The results of this investigation are shown in Table 5 and discussed in the following sections.

(a) Heat Transfer Correlation

The overestimation of the pin sheath temperature is consistent with results published by Yetman and Sanderson [2]. The over-estimation of the pin temperatures was attributed to an underestimation in the default post dry-out (PDO) heat transfer coefficient (Groeneveld-Delorme). Yetman and Sanderson [2] were able to obtain improved agreement using the Bromley correlation for PDO conditions, although the Bromley correlation tends to underestimate peak sheath temperatures. Application of the Bromley correlation in this study resulted in a greatly improved average maximum sheath temperature, but with a much greater axial variation in temperature (see the standard deviations in Table 5). The agreement between the calculated and measured sheath temperatures depends on the axial location. The Leung and Groeneveld PDO table was later made available in CATHENA MOD-3.5c/Rev 0 to improve predicted heat transfer under post dry-out conditions. The Leung and Groeneveld PDO table was therefore examined and compared with the default Groeneveld-Delorme correlation under a number of conditions (Table 5). The results in Table 5 show for each of the cases using the Leung and Groenveld correlation, a lower average maximum temperature is calculated than with the Groeneveld-Delorme correlation, however higher sheath temperatures (> 300°C) are calculated between 50 and 100 s. With the Groeneveld-Delorme correlation, all top pin temperatures dropped to the measured values of 250°C by 50 s.

(b) Flow Regime Transition

Under default conditions, the flow regime in the channel is single-phase liquid at the beginning of the transient, and quickly becomes stratified with a small amount of water (between 5 to10% by volume) remaining on the bottom of the channel. Simulations were performed in which the flow regime during the transition from single-phase liquid was set to mixed instead of being allowed to stratify (Table 5). For all of the cases examined with the flow regime fixed in mixed, the average maximum sheath temperature was lower than the average maximum sheath temperature calculated with the default flow regime transitions. Fixing the flow regime in mixed, with all other parameters set to default conditions, reduced the average maximum temperature to 555°C, however, a large standard deviation (axial variation) in the temperature was maintained (30°C).

(c) Break Conditions

Reducing the break diameter by 1.2 mm and changing the break discharge coefficient had little impact on the average sheath temperatures (calculating an average maximum axial temperature of 582°C, with a standard deviation of 40°C, Table 5); however, together with the flow regime set to mixed, changing the break conditions lowered the average maximum sheath temperature to 550°C and reduced the standard deviation in the average maximum sheath temperature to 18°C (see Figure 12). The calculated inlet and outlet channel flows for this case was also the closest to the measured flows (compare Figures 7 and 13, and 8 and 14).

Examining the effect of two heat transfer correlations, the transition flow regime and the break conditions, the following points were determined:

1. the Bromley correlation for PDO conditions improved the agreement of the average maximum sheath temperature determined from the simulation with the experimental average maximum temperature, but at the expense of a greater axial variation in the peak sheath temperatures.
2. although the Leung and Groeneveld PDO look-up tables resulted in lower peak sheath temperatures (closer to the measured temperatures) than the Groeneveld-Delorme correlations, the sheath temperatures later in the transient calculated with the Leung and Groeneveld correlations were much higher than the measured temperatures.
3. improved agreement with measured inlet/outlet channel flows was obtained if the calculations are performed under mixed flow conditions with a 15% smaller break area than that quoted in the experiments, and the break discharge coefficient changed from 0.3 to 0.8 at 14 s.
4. improved agreement with measured channel flows gave improved agreement of the calculated sheath temperatures with measured temperatures. The average maximum sheath temperature calculated under mixed flow conditions with modified break conditions was reduced to 550°C from 581°C calculated under default conditions. The standard deviation of the average maximum axial temperature was also reduced from 30°C to 18°C compared to 10°C from the measured data.

Overall, the best agreement between calculated axial sheath temperatures was obtained with the Groeneveld-Delorme correlation, with the flow regime set to mixed, the break diameter reduced to 13.8 mm and a variable break discharge coefficient (0.3 for transient time < 14 s, and 0.8 for transient time > 14 s). Improved agreement between the measured and calculated sheath temperatures was obtained with the modified break discharge coefficient and discharge area under mixed flow conditions because agreement between the calculated and measured channel flows was improved. The error in the experimental discharge break area is within 0.1% and the error in the discharge coefficient is at most ±10%, so the required changes in break area and discharge coefficient suggests the discharge model under these conditions overestimates the discharge. Validation of the discharge model has established an uncertainty of ±16% in the mass flow. In the study reported in this paper, changing the discharge conditions resulted in a 10% increase in the mass flow from the default calculation after the first three seconds of the transient. The 10% change in mass flow required to achieve agreement in the channel flows is well within the uncertainty of the discharge model.

Although good agreement in the channel flows was obtained with the modified break discharge conditions, the average maximum axial sheath temperature determined from the simulation was still higher than the experimental average maximum temperature by as much as 42°C. To obtain further improvement in the agreement between the calculated and measured sheath temperatures early in the transient, the heat transfer correlations for these conditions should be examined.

Summary

This exercise examined the ability of CATHENA to predict thermalhydraulic conditions (pre-test simulation) in an RD-14M critical break experiment and the ability of CATHENA to calculate (post-test simulation) the thermalhydraulic conditions given a detailed description of the experiment. The major changes between the pre- and post-test simulations were

a) FES channel power histories,
b) primary pump RPM rampdown curves
c) header 8 break valve delay time
d) initial conditions in header pressure and temperature

The major differences between the pre- and post-test results were

a) at the two locations examined, the maximum post-test peak sheath temperatures were 10°C lower than the pre-test peak sheath temperatures
b) the flow in test section 14 reversed 1.1 s later in the post-test simulation. This can be attributed to the application of a delay time in the break valve opening in the post-test simulation.

The peak sheath temperatures in the pre-test simulation results were not significantly reduced in the post-test results. Therefore, the power pulse histories, primary pump rampdown curves, the secondary side boundary conditions, and the header initial conditions in the pre-test simulation were good approximations to the post-test simulation conditions.

The peak sheath temperatures for the top pins at the end of test section 14 calculated under default conditions (heat transfer correlations, channel flow regime and discharge conditions), were as much as 108°C higher in the post-test simulation than in the experiment. This corresponded to an average maximum sheath temperature 73°C higher in the simulation than in the experiment, or 15%. However, when the discharge conditions and channel flow regime early in the transient were modified to improve the agreement between measured and calculated channel flows, the average maximum sheath temperature using the default Groeneveld-Delorme correlation overestimated the measured average temperature by only 42°C, or 8.3%. The change in discharge conditions, however, resulted in a 10% change in discharge flow which is well within the uncertainty of the discharge model. These results demonstrate the sensitivity of the pin temperatures to discharge flow. Further improvement in the agreement between calculated and measured sheath temperatures would require modified heat transfer correlations under the conditions examined.

Acknowledgements

The author greatly appreciates the helpful discussions with B.N. Hanna, J.R. Buell and J.P. Mallory which brought the work presented in this paper to completion.

References

[1] Hanna, B.N, "CATHENA: A Thermalhydraulic Code for CANDU Analysis," Nuclear Engineering and Design (180), pp 113-131 (1998).

[2] Yetman, E.J.M., and T.V. Sanderson, "Pre- and Post-Test CATHENA Simulations for RD-14M Critical Break Experiments," Presented at the 5th International Conference on Simulation Methods in Nuclear Engineering, September 8-11, Montreal 1996

[3] Ingham, P.J., A.J. Melnyk and T.V. Murray, "Two-Phase Flow Stability Experiments in RD-14M," Presented at the 12th Annual Conference of the Canadian Nuclear Society, June 9-12, 1991, Saskatchewan.

Table 1
Nominal Conditions for Test B9903

PRIMARY SYSEM	
Nominal Channel Power	0.74 MW/pass
Primary Side Pressure	10.1 MPa (g)
Primary Flow	3.65 L/s
Break Size	15-mm diameter (at Header 8)
SECONDARY SYSTEM	
Secondary Side Pressure	4.5 MPa(g)
Boiler Level	55% in both boilers
Feedwater Temperature	153°C

Table 2
Sequence of Events for Test B9903

Time (s)	Event
0.0	Surge tank isolated
10.0	Header break initiated
10.2	Power ramp to peak power in test section 14 (TS14) initiated.
12.0	Primary-pump rampdowns initiated
176.9	Data collection in experiment stopped

Table 3
Initial Conditions for Pre-test Simulation of B9903

PRIMARY SYSTEM		
	Pressure (MPa)	Temperature (°C)
Inlet Header 8	10.84	250.2
Inlet Header 6	10.86	250.2
Outlet Header 5	10.10	300.5
Outlet Header 7	10.08	300.5
Test Section 9 and 14 Inlet Flows (L/s)	3.46	
Test Section 9 and 14 Outlet Flow (L/s)	3.90	
Test Section 9 and 14 Channel Power (Boundary Conditions)	0.74 MW	
SECONDARY SYSTEM		
Feedwater Flows (Boiler 1 and 2) (kg/s)	0.34	
Boundary Conditions:		
Pressure (Boiler Outlet)	4.5 MPa	
Feedwater Temperature (Boiler Inlet)	180 (°C)	
Boiler Level (55%)	840 mm	

Table 4
Calculated Post-test and Measured Initial Conditions for Test B9903

PRIMARY SYSTEM				
	Measured		Calculated	
Inlet Header 8	10.54 MPa	245.6°C	10.92 MPa	249.7°C
Inlet Header 6	10.56 MPa	253.2°C	10.94 MPa	249.6°C
Outlet Header 5	9.71 MPa	298.7°C	10.10 MPa	298.1°C
Outlet Header 7	9.70 MPa	298.9°C	10.08 MPa	298.2°C
Test Section 9 Inlet Flow (L/s)	3.75		3.63	
Test Section 9 Outlet Flow (L/s)	4.17		4.08	
Test Section 14 Inlet Flow (L/s)	3.67		3.63	
Test Section 14 Outlet Flow (L/s)	4.10		4.08	
Test Section 9 and 14 Channel Power (Boundary Conditions)	746		746	

Table 5
Average Maximum Top Pin Sheath Temperatures

			Conditions			
Time (s)	Average Maximum Temp (°C)	Standard Deviation (°C)	Heat Transfer Correlation	Flow Regime Transition	Break Diameter (mm)	Break Discharge Coefficient
16.7	508	10	Experiment	Experiment	15.0	Experiment
16.9	581	30	Groeneveld-Delorme (Default)	Stratified (Default)	15.0	0.61 (Default)
16.5	507	84	Bromley	Stratified (Default)	15.0	0.61
17.8	555	31	Default	Mixed	15.0	0.61
17.5	564	17	Default	Mixed	13.8	0.61
18.3	560	18	Default	Mixed	13.8	0.3 (0 to15 s) 0.61 (>15 s)
18.3	582	40	Default	Stratified (Default)	13.8	0.3 (0 to15 s) 0.61 (>15 s)
17.6	600	33	Default	Stratified (Default)	13.8	0.61
17.6	550	18	Default	Mixed	13.8	0.3 (0 to14 s) 0.8 (>14 s)
16.7	566	36	Leung-Groenveld	Stratified (Default)	15.0	0.61
16.9	567	45	Leung-Groenveld	Stratified (Default)	13.8	0.3 (0 to14 s) 0.8 (>14 s)
17.5	540	15	Leung-Groenveld	Mixed	13.8	0.3 (0 to14 s) 0.8 (>14 s)

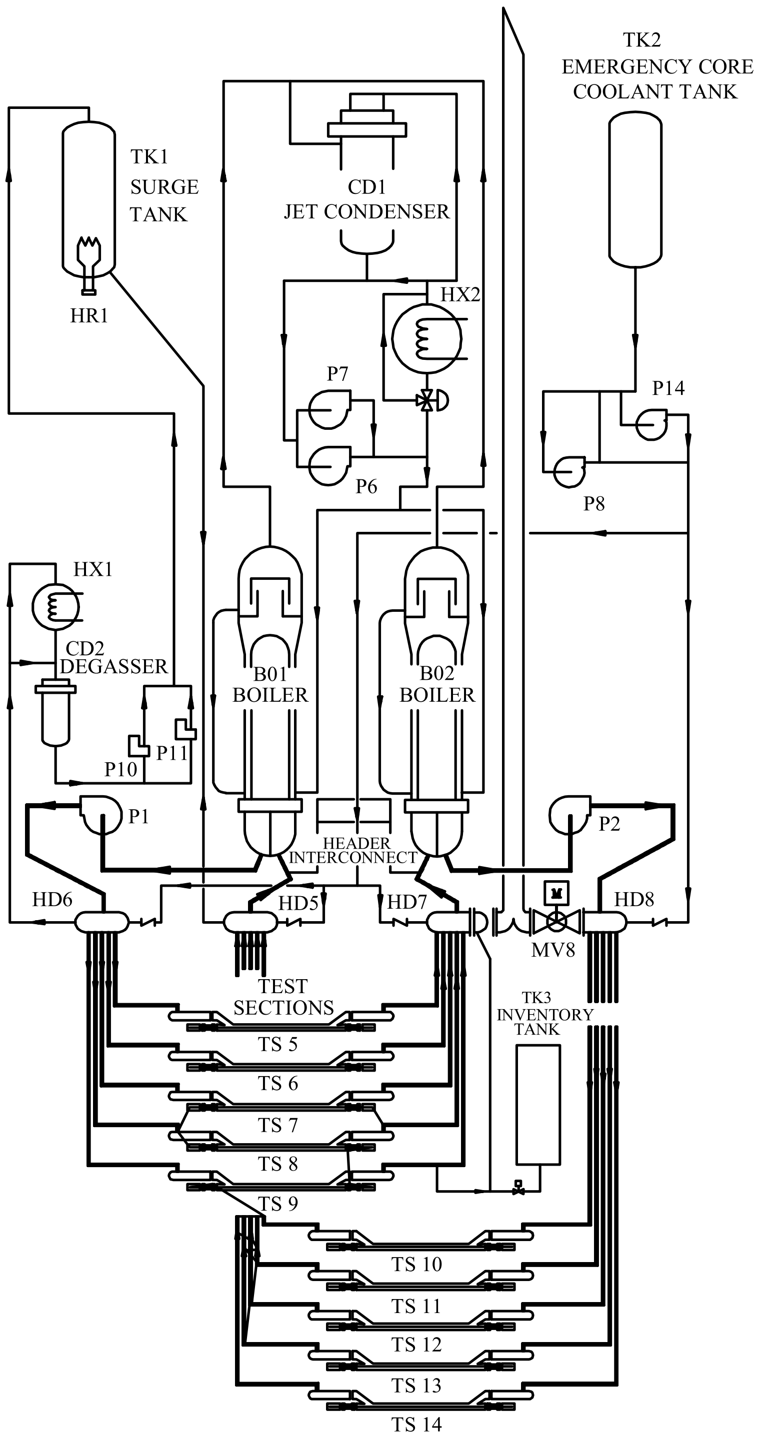

Figure 1: Schematic of RD-14M Facility

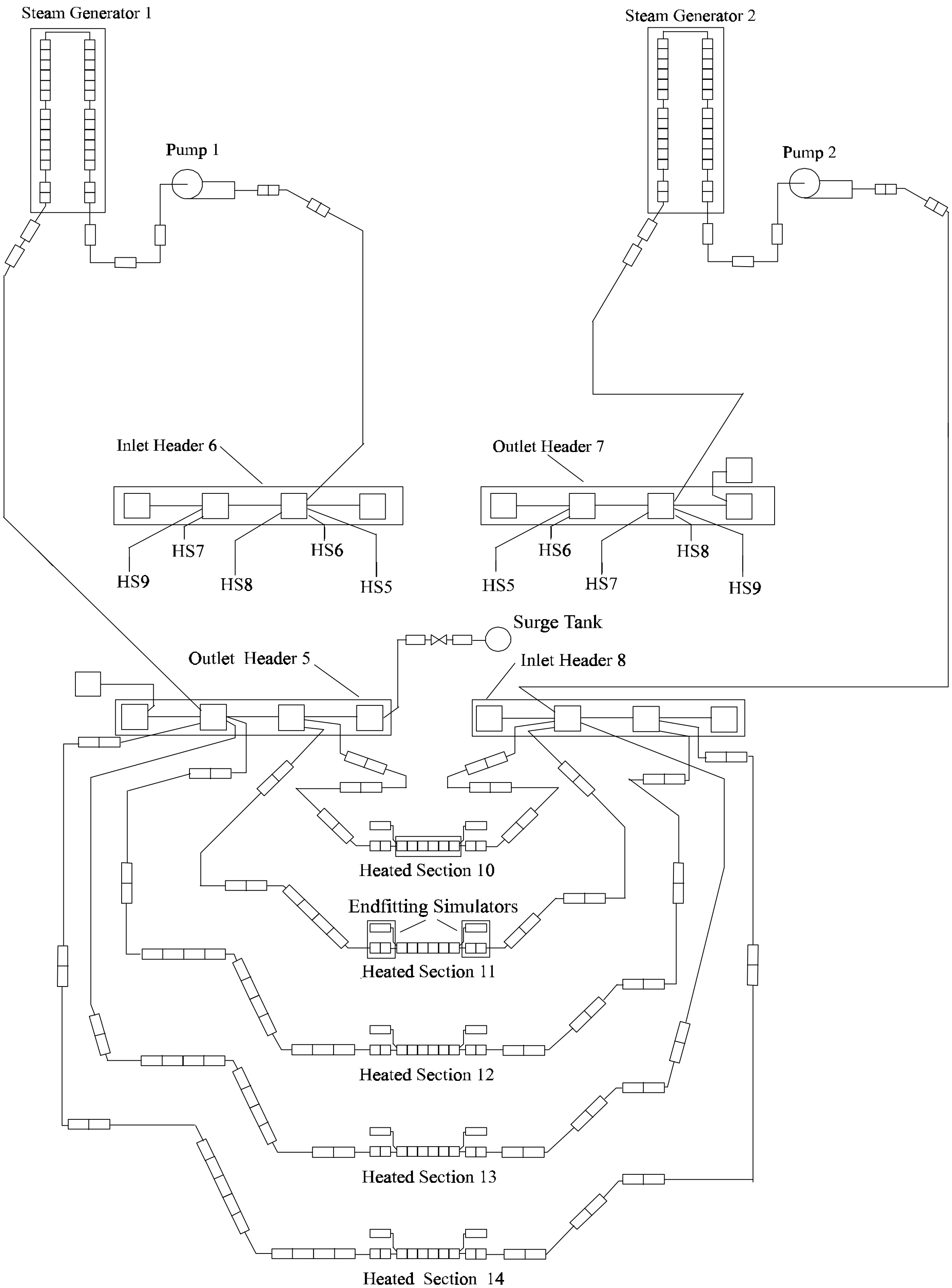

Figure 2: CATHENA Idealisation of Primary Side

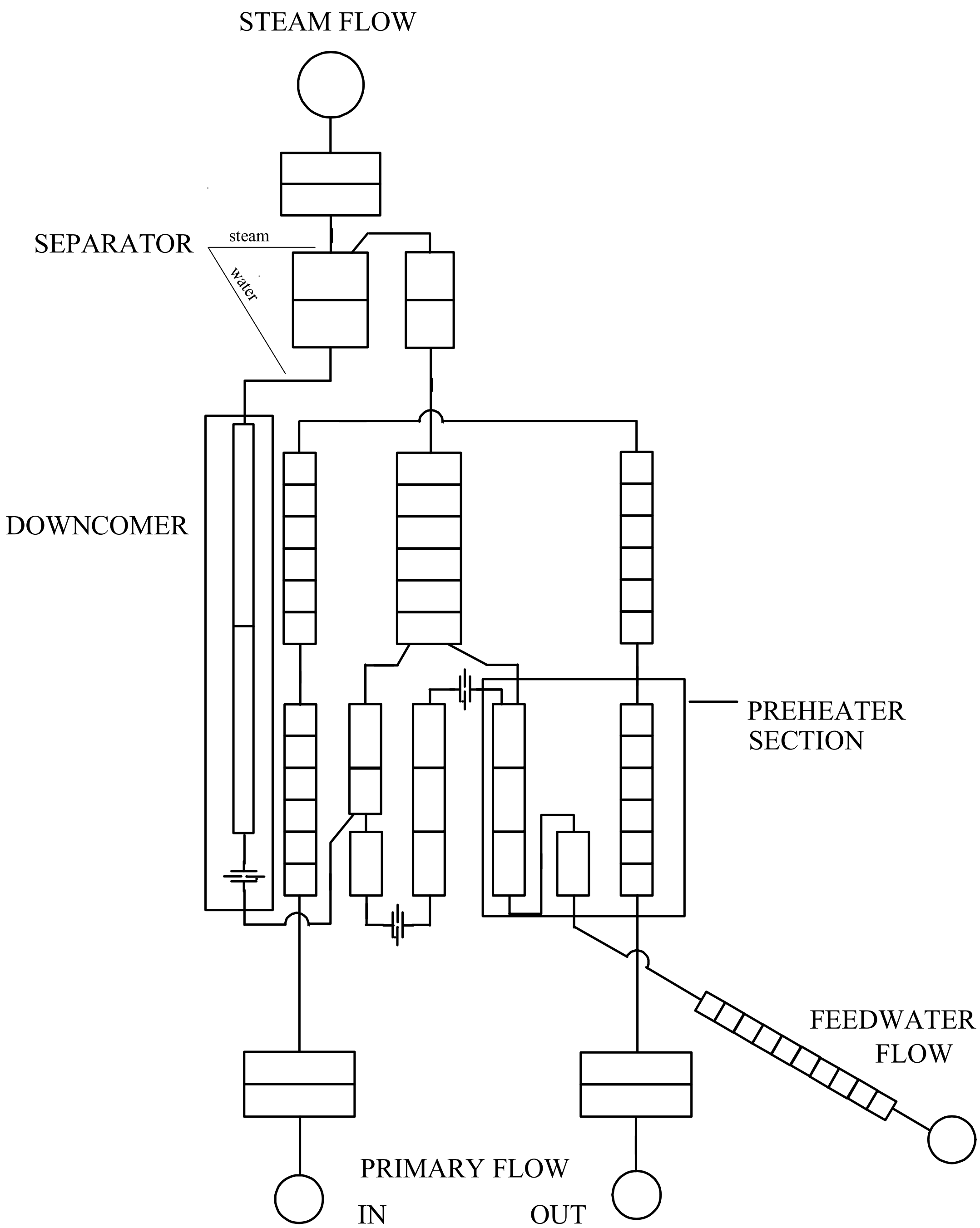

Figure 3: CATHENA Idealisation of RD-14M Secondary Side

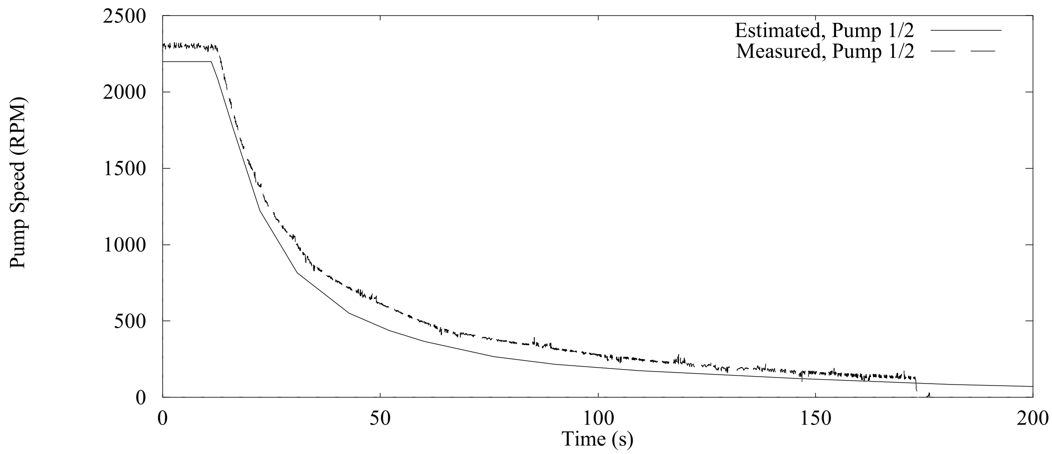

Figure 4: Estimated and Measured Primary Pump Rampdown Curves used as Boundary Conditions for Pre- and Post-Test Simulations respectively

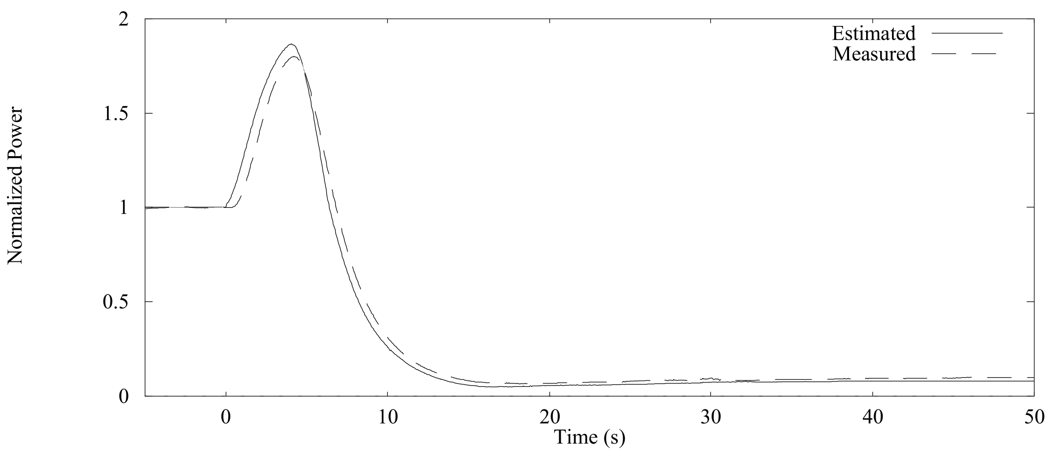

Figure 5: Pre-test Estimation and Measured Power Input for Test Section 14

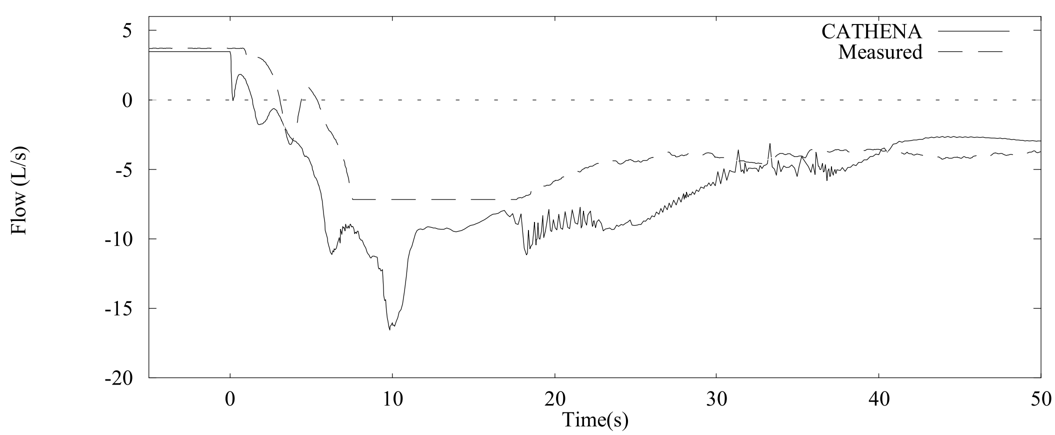

Figure 6: Pre-test and Measured Test Section 14 Inlet Flow

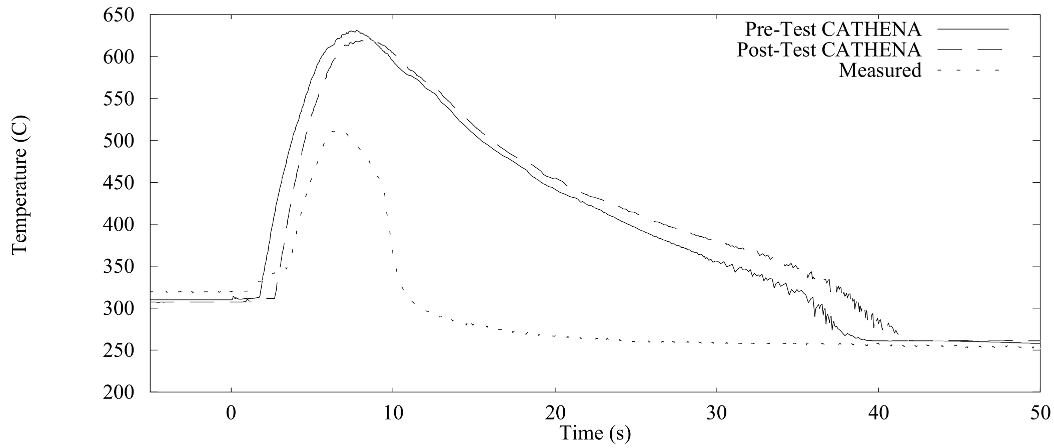

Figure 7: Pre- and Post-test and Measured Transient of Sheath Temperature for Top Pin, End of Test Section 14

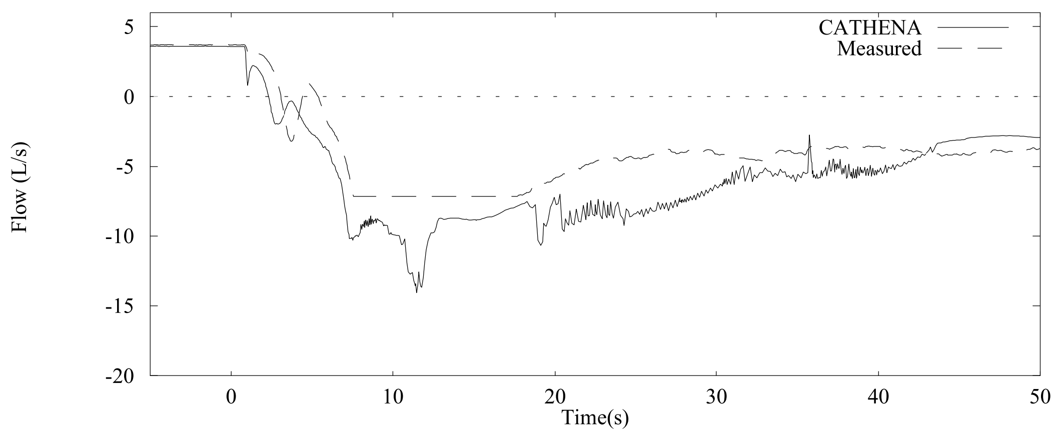

Figure 8: Post-test and Measured Test Section 14 Inlet Flow

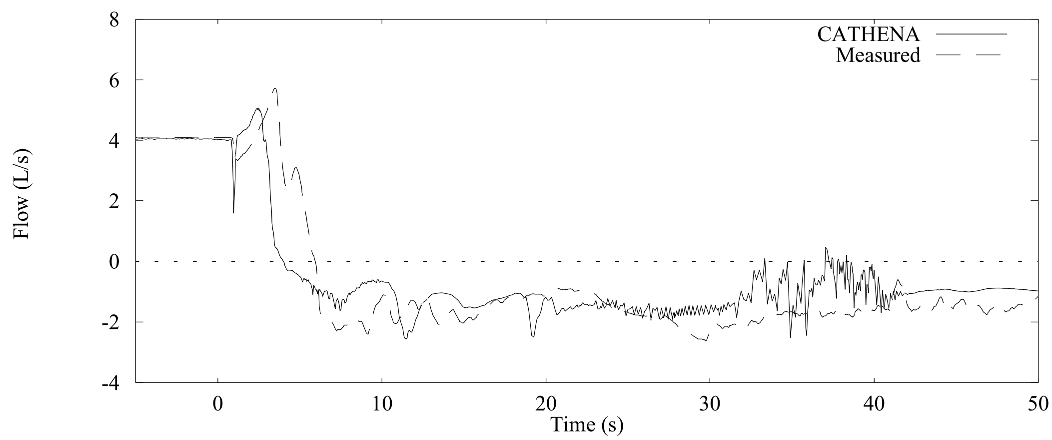

Figure 9: Post-test and Measured Test Section 14 Outlet Flow

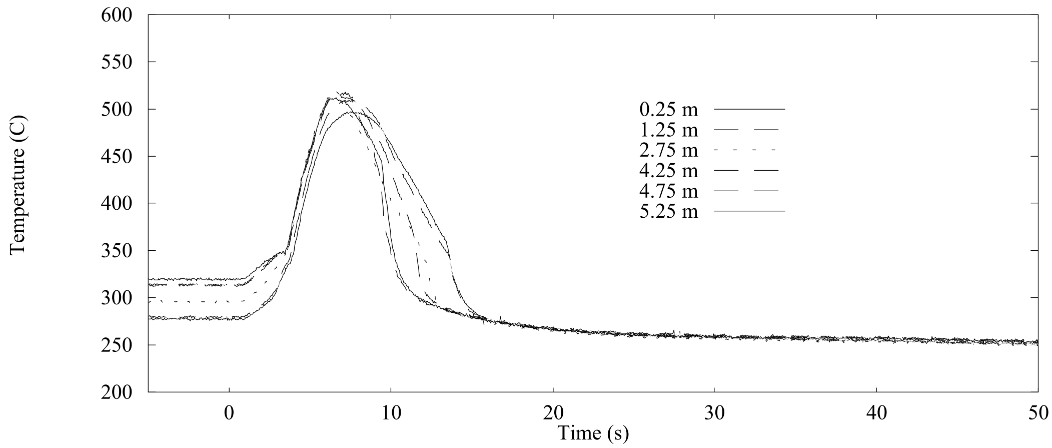

Figure 10: Measured Top Pin Sheath Temperatures for Test Section 14. Locations indicate distances from Inlet.

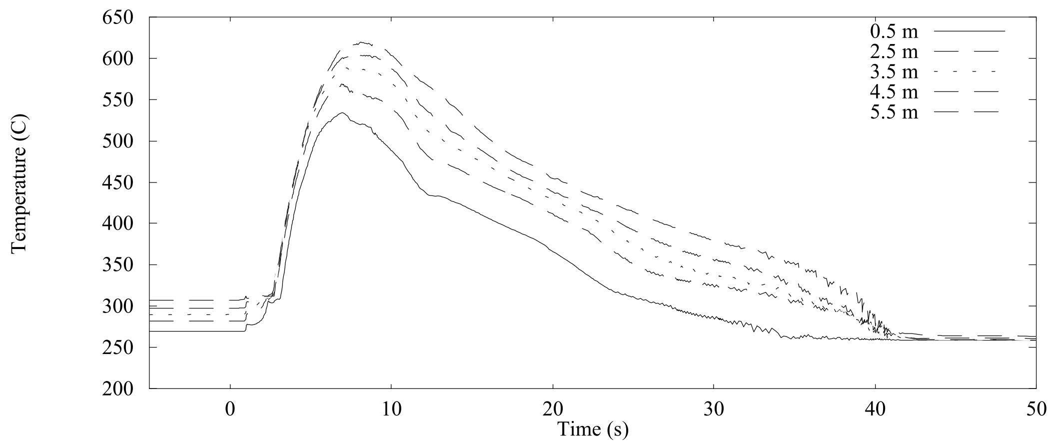

Figure 11: Calculated Top Pin Sheath Temperatures for Test Section 14 using Default Parameters

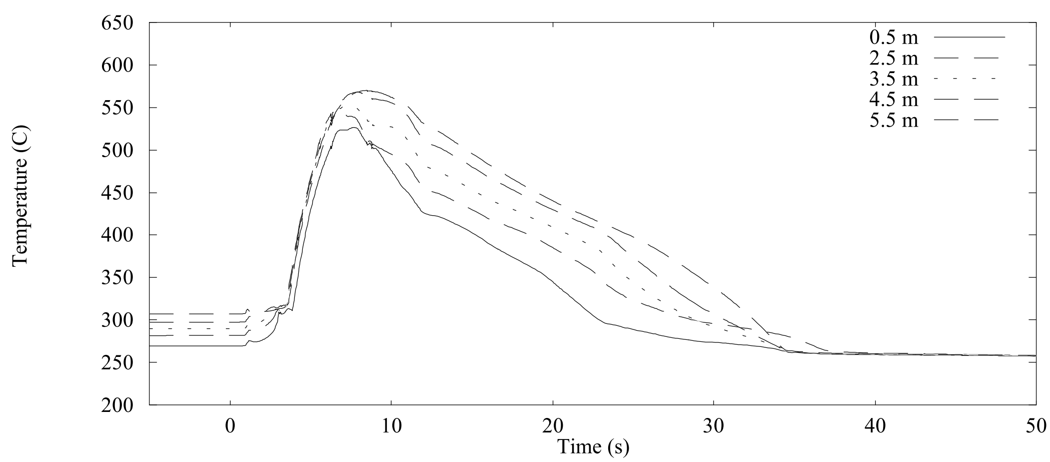

Figure 12: Calculated Top Pin Sheath Temperatures for Test Section 14 using Default Heat Transfer Correlations with Mixed Transition Flow Regime and Modified Break Conditions (13.8 mm break diameter and Variable discharge Coefficient).

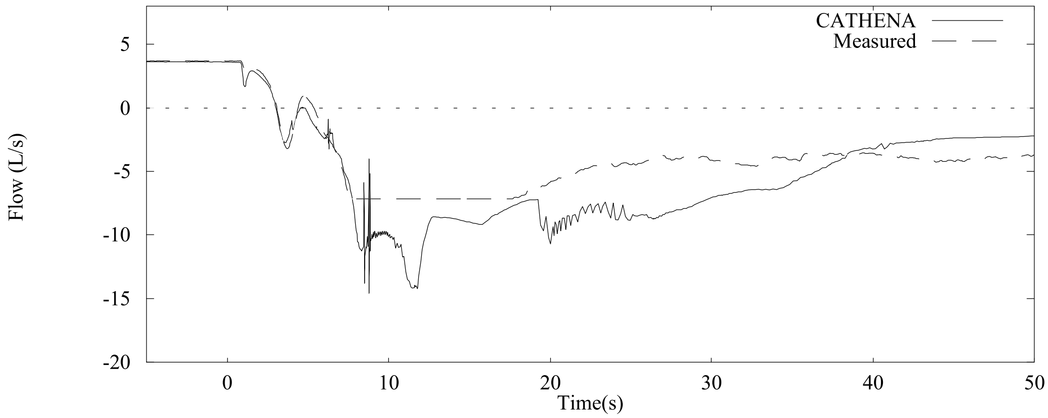

Figure 13: Post-test and Measured Test Section 14 Inlet Flow with Transition Flow Regime set to Mixed and Modified Break Conditions (13.8 mm break diameter and Variable Discharge Coefficient).

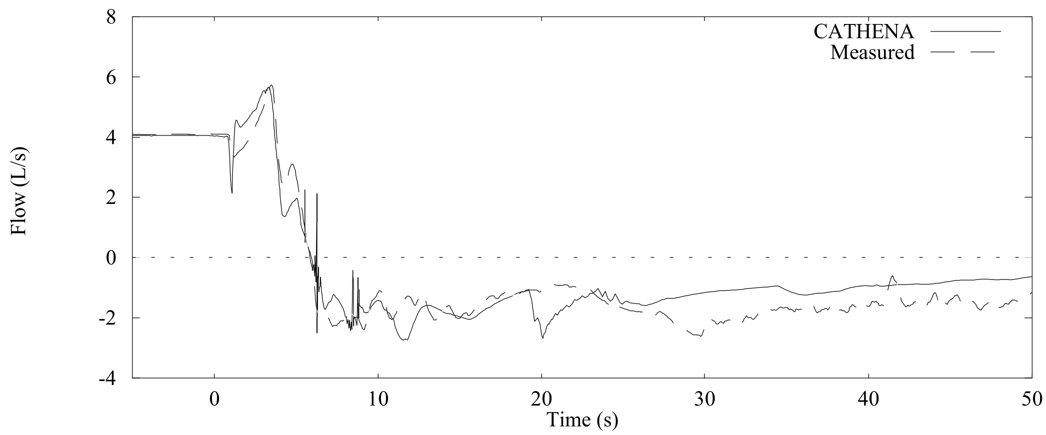

Figure 14: Post-test and Measured Test Section 14 Outlet Flow with Transition Flow Regime set to Mixed and Modified Break Conditions (13.8 mm break diameter and Variable Discharge Coefficient).